On feasibility of longitudinal characterisation of photonic structures via transverse excitation of whispering gallery modes

M. Bukshtab

Remote side excitation of whispering gallery modes in a photonic crystal fibre reveals longitudinal properties of its intra structure usually requiring a long propagation length and endface access. By tuning the excitation to maxima of observed morphology resonances, initiating axially expanding whispering gallery modes in the fibre cladding and in its microstructure, characteristic spectral windows resembling ones at the fibre longitudinal transmission are observed. This outcome opens up possibilities of remote characterization of rotationally-symmetric photonic structures in situ and in locations only assessable via side excitation using external light beams.

Introduction: The photonic crystal structures [1], such as antiresonant fibres and waveguides [2, 3], offer physical properties allowing to expand capabilities of silica fibres [4]. Excitation of whispering gallery modes (WGMs) in a fibre cladding enabled characterization of the fibre diameter with sub-nanometer level of sensitivity [5, 6]. Recently, we have reported direct side-coupling of light to internal fibre microstructure from WGMs excited in the fibre cladding, which permitted observing banded spectral resonances associated with distinct capillaries of the fibre [7]. At the same time, direct excitation of WGMs in individual capillaries of the antiresonant fibres to characterize their dimensions were also described [8]. Here we report for the first time on the observation of characteristic spectral windows associated with longitudinal propagation of light inside a hollow core fibre via side excitation of axially extending WGMs in fibre capillaries and its cladding, enabling to sense resonant features of a fibre.

Observations: The goal of our study was to investigate the possibility of external characterization of a hollow core fibre in an assembled preform, in the latter homothetic extension into a fibre cane, and while drawing the fibre. In setting up a system for characterization of fibres and canes we intended to use remote light beams versus phase-matched excitation by a taper [9] to enable detached coupling of light into a fibre microstructure. The diverging-beam excitation of cladding modes enhanced spreading of internally reflected rays in a fibre and filling-in capillaries of its structure (see Fig. 1). Since the propagation constant for a silica fiber is always closest to that of the lowest radial mode number for a whispering gallery mode (WGM), leaking higher order cladding modes were broadly guided into all antiresonant elements, such as the inner and outer capillary tubes. Spectral maxima of WGM resonances in a fibre cladding/capillaries $|r|^2$ and transmission resonances past the fibre $|t|^2$ are given by relations [10]:

$$|t|^2 = \frac{(\alpha - |t|)^2}{(1-\alpha|t|)^2}; \qquad |r|^2 = \frac{\alpha^2(1-|t|)^2}{(1-\alpha|t|)^2}. \qquad (1)$$

Here α, t are the inner-ring circulation and complex transmission factors.

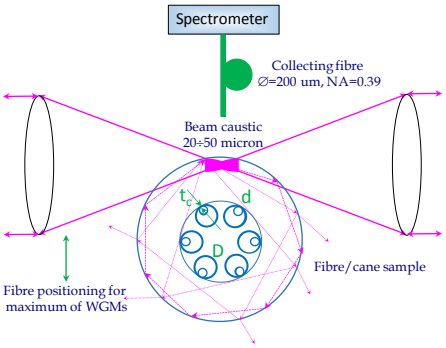

Fig. 1 *Schematic illustration of side excitation: either a left or right beam is focused onto a periphery of fiber while the latter position is moved into the beam (vertical arrow) until the maximum intensity of WGM is reached*

Fig. 1 shows an enlarged profile of Nested Antiresonant Nodeless Fibre (NANF) [11] with outer/inner tubes of diameter D/d at the capillary wall thickness t_c. The optical system assembled to investigate fibre properties via side scattering is depicted in Fig. 2. Our intent was to observe changes of birefringence in a fibre cross section in transmitted plus reflected light [12] similarly to two-beam interferometric conception applied in Ref. [6].

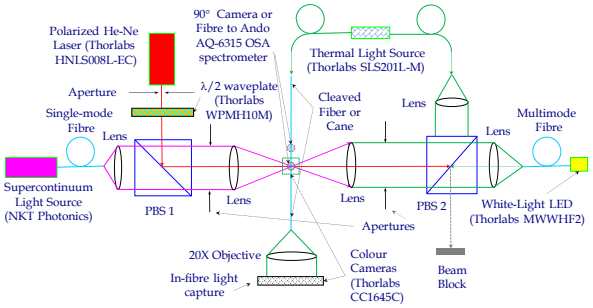

Fig. 2 *Experimental system for side excitation of WGMs in fibre structure via registration of 90-degree scattering: PBS – polarization beam splitter*

Distinct emission sources: coherent, partially coherent, and spontaneous (Fig. 2), were consequently coupled into a fibre or cane. Observations of scattering at maxima of WGMs excitation revealed interference patterns and banded spectral resonances linked to fibre microstructure (Figs. 3, 4).

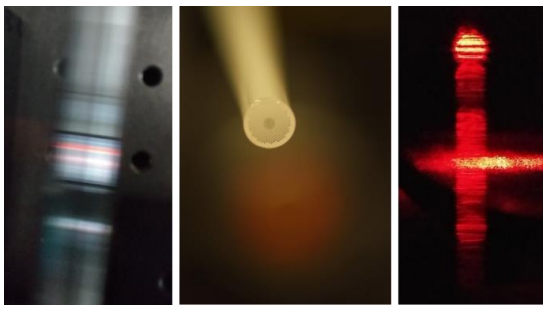

Fig. 3 *White light interference in photonic-bandgap-fibre cane resembles theoretical WGM-interference estimate [13] for broadband light (a); red resonant beam exits a cane endface (b); fiber interference, laser light (c)*

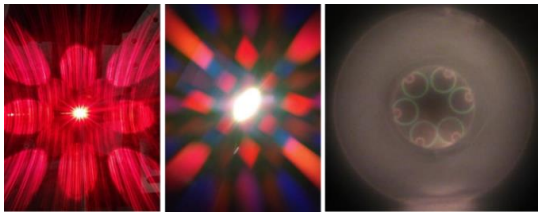

Fig. 4 *Intra capillary tubes of NANF fibre (a) overlap resonant scattering on a fibre as a long cylinder [14], spectrally banded resonances observed in 7-capillary Antiresonant Nodeless Fibre (b), and green/red resonances in outer/inner tubes of NANFb fibre (c) at side excitation, white LED light*

Initially, a 90° camera or collecting spectrometer fibre (see Fig. 2) were placed along a tested fibre away from 90° position over axially-extending WGM pattern until the maxima of intensity were found always at 90°. To observe images of Figs. 3, 4, the 20X capture objective and colour camera (Fig. 2) were used, or wide-angle and high resolution cameras. Following the observed retention of side-scattered light inside silica capillaries of intrafibre structures in diverse types of fibres, for example confirmed by low-intensity red light beam longitudinally exiting the cane or green and red outer/inner-tube microstructure resonances, one would expect bottle WGM modes, for which light spirals back and forth along the axis of a cylindrical resonator with thickness variations of the adiabatically drawn fibre [15], to exhibit a resemblance to transmission properties of the fibre.

Spectral measurements: Maxima of WGM resonances confirmed via 90° scattering visually or by a spectrometer were replicated at spectral studies of side transmittance and scattering. Low loss 1.3-dB/km NANF [16] was

tested versus a Solid (coreless) Fibre (SF), a single-capillary Tube Fibre (TF), single-mode fibre SMF-28 (Corning, Inc.), and three experimental NANFs with two outer tubes touching or not touching each other. Fig. 4, *c* depicts a version NANFb with tubes partially touching, compared to a fully touching NANFa and not-touching section NANFc of that fibre. All spectrums below were obtained via 200-micron multimode fibre placed at the 15.4 mm gap above a studied fibre, irradiated by visible light from either the Supercontinuum or a combined source – comprising Thermal plus LED lights. To integrate sharp extrema of WGM interference in fibre cladding all measurements were performed at a 10-nm spectral resolution.

Fig. 5 shows 90°-scattering spectrum of NANF fibre at the maximum of visible WGMs via side scattering in Supercontinuum light, revealing relatively narrow green and red resonance peaks, likely pointing to its all equivalent capillary pairs. Fig. 6 spectrum of NANFb fibre with touching tubes depicts multiple resonances in the green and red spectral windows and the leakage of light between 550 – 600 nm due to two joint capillaries.

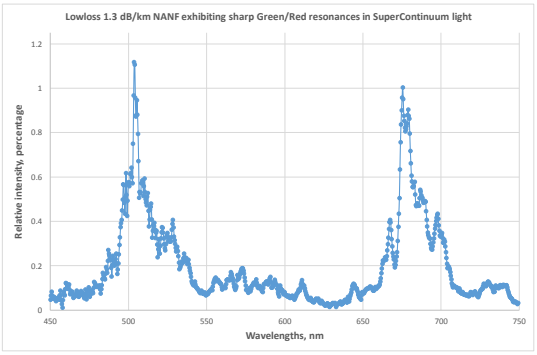

Fig. 5 *Observed spectral resonances measured for NANF sample via side excitation of whispering gallery modes by visible Supercontinuum light*

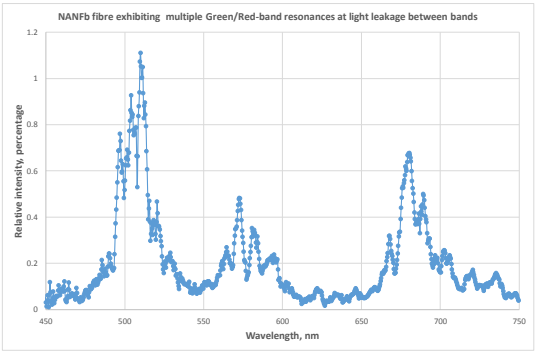

Fig. 6 *Multi-wave resonances of NANFb sample in Supercontinuum light*

Further studies via spectrally stable combined LED–Thermal source of Fig. 2 helped removing ambiguities associated with lower reproducibility of Supercontinuum source, while lacking the phase matching for partially coherent beams among individual cladding and microstructure resonatorsand reducing penetration of spontaneous light into a fibre. The combined source had LED-dominated spectral content from 400 to 700 nm with the thermal source adding its intensity contribution between 700 and 750 nm.

Side transmission spectrums T_{rs} of Fig. 7 were obtained at exactly same individual fibre positions as 90° scattering via the maximum intensity of WGM resonances. All transmittance values are in absolute scale referred to the combined source intensity. The spectrums here are zoomed into the region of three attenuation windows observed for blue/green wavelengths while no other bands, such as red resonances of Figs. 3, 4 were observed.

Fig. 8 shows 90° scattering spectrums S_{rs} of tested fibres at the absolute scale of scattering projected for 2π-space from 0.0130-radian solid angle. Subsequent spectrums of intrafibre capture in Fig. 9 were calculated from transmittance and scattering as $C_{rs} = 1 - T_{rs} - S_{rs}$. Three spectral windows seen as dips in capillary-fibre spectrums resemble antiresonant properties for 11th 10th and 9th order of the fibres resonant transmission [3]. Fitting central wavelengths of 517.0, 465.3, 423.0 nm to one effective pathlength thickness of 4653.00 nanometres predicts 1551-nm centre wavelength of the 3rd order. Based on 1170±29 nm wall thickness for outer capillaries of the NANF measured in Ref. [16], the design wavelength for its 2nd window is 1551.4-nm, only 0.4 nanometer off the value measured above.

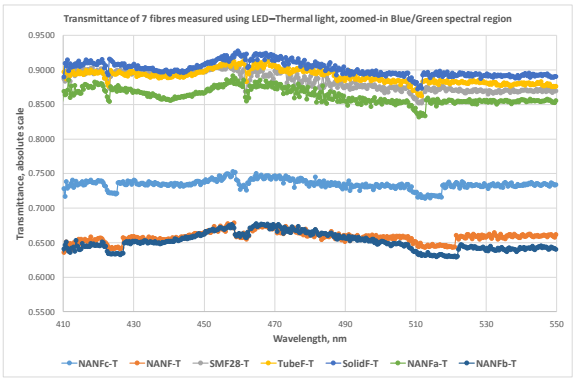

Fig. 7 *Transmittance spectrums of compared fibres in spontaneous light*

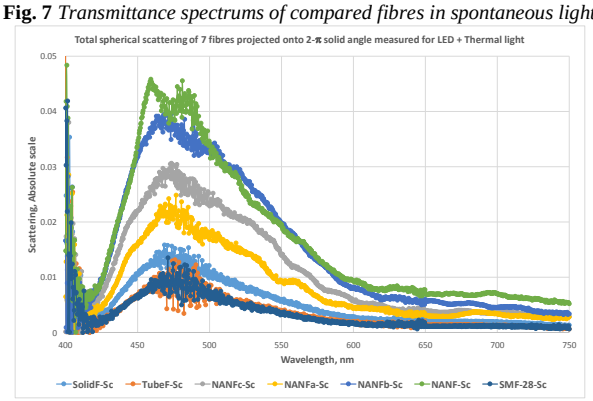

Fig. 8 *Total 2π-scattering spectrums of seven fibres, LED–Thermal light*

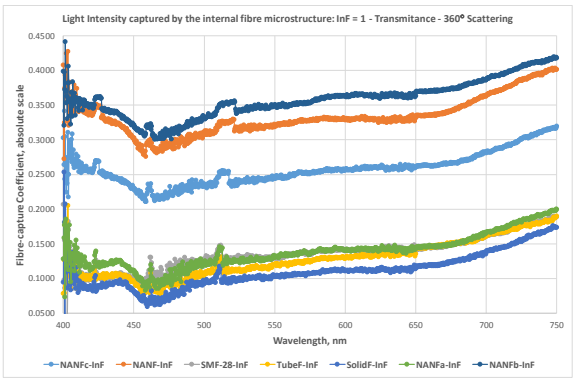

Fig. 9 *Perceived fibre capture spectrums of all fibres, LED–Thermal light*

To verify the observed phenomena, best samples NANF, NANFb, and NANFc were remeasured at 3-point averaging of OSA signal acquisition. Enhanced WGM transmittance and scattering spectrums of Fig. 10 reveal a notably broad 512.00–538.95 nm antiresonant window for the NANF, intended for CL-band transmission, at equal coordinates for transmission and scattering. Intrafibre capture spectrums of Fig. 11 were obtained as ones of Fig. 9 via 3-point averaged transmittance values of Fig. 10 and correlated 3-point total scattering spectrums, similar to the ones of Fig. 8.

For 3-point spectrums all 10th order dips were much narrower, fading away since not supported by the antiresonant fibre design, and thus were ignored in further analysis. Since the fibre capillary wall thickness t_{ant} had been optimized to be antiresonant for minimal propagation losses [3, 17]: $t_{ant}\sqrt{n^2-1} = (2k+1)\lambda;\ k = 0,1,2\ldots$, the beginning and the end of 6th and 5th windows, or the 11th at k=5 and 9th at k=4 orders, were utilized to calculate the start and end of other windows up to 1st one. Afterward, the

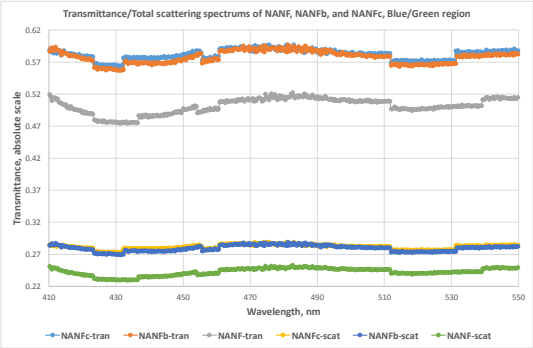

Fig. 10 *Enhanced WGM-mode transmittance and scattering spectrums*

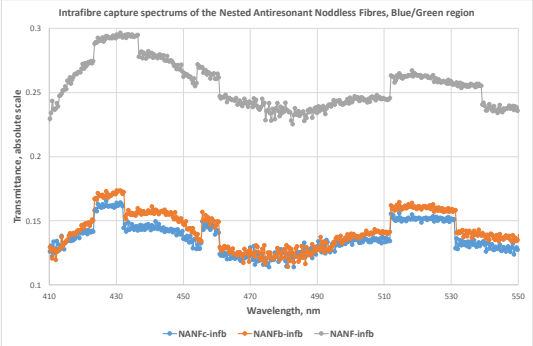

Fig. 11 *Enhanced WGM-mode intrafibre capture spectrums of best fibres*

coordinate of a window centre along with values of refractive index n_λ were applied to compute the mean thickness t_{ant} of capillary walls. Based on 423.45–436.4-nm 6th window, t_{ant1}=1101.22 nm, and on 5th one, t_{ant2} =1109.99 nm, the mean thickness for NANF fibre was t_{ant} =1105.6±4.4 nm, pointing to centres of 2nd and 1st transmission windows at 1535.6±6.5 nm and 4541.4±18.1 nm. The actual design thickness of capillary wall of NANF measured in Ref. [16] of 1170 nm had been held for its outer tubes, while the inner tube wall thickness was reduced to 1080 nm at the average of 1125±30 nm, only 20 nanometres higher our result above. The centre of its 2nd longhaul transmission window measured for 500-m sample had also shifted farther away from our 1535.6 nm evaluation to near 1450 nm.

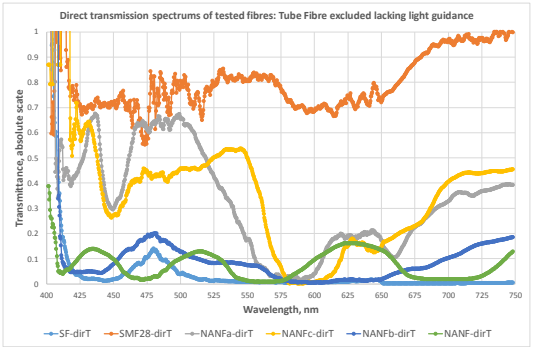

Fig. 12 *Cutback transmittance measurements for fibres of light guidance*

Direct transmission measurements (Fig. 12) were made by the cutback method. The exactly same fibre samples of 25±5 cm length were used for long sections, cut down to 4±1 cm for short ones. Each section was held on 3-D positioning stage, light coupling to which was maximized before the start of a measurement cycle via OSA readings, at cutback performed on the stage unmoved. The results for shorthaul fibre transmission measurements confirm NANF fibre to be truly antiresonant with centres of three visible windows (4th is over 750 nm) at 435.0, 515.5, and 627.5 nm. The first two windows match 6th and 5th ones of WGM studies within 5–10 nm, the reason for absence of 4th window in WGMs spectrum is unclear. Among other samples NANFb fibre of distinct colour resonances but showing out-of-band leakage (Fig. 4, c and Fig. 6) behaved closest to NANF, with the eminent lowest loss for SMF-28. One transmission band centred at 479.8 nm for Solid Fibre could be indicative of its overall size.

Conclusion: Detecting characteristics of longitudinal structure properties at transverse excitation of whispering gallery modes in hollow core fibres offers potentials for remote evaluation of otherwise inaccessible samples.

Acknowledgements: The author wishes to thank J. R. Hayes, P. Horak, T. Bradley, Y. Chen, H. C. Mulvad, R. Slavik, F. Poletti, D. J. Richardson for helpful suggestions and support, and also O. Aktas, G. T. Jasion, S. R. Sandoghchi, W. Zhu. Funding for this work is provided by the UK Engineering and Physical Sciences Research Council (EP/P030181/1).

M. Bukshtab (University of Southampton, Southampton, SO17 1BJ, UK)

E-mail: M.A.Bukshtab@soton.ac.uk

References

1. Yablonovitch, E.: 'Photonic band-gap structures', JOSA B, 1993, **10** (2) pp. 283–295
2. Knight, J. C., Birks, T. A., Russell, P. St.J., Atkin, D. M., 'All-silica single-mode optical fiber with photonic crystal cladding', Opt. Lett., 1996, **21** (19), pp. 1547–1949
3. Duguay, M. A., Kokubun, Y., Koch, T. L., Pfeiffer, L.: 'Antiresonant reflecting optical waveguides in SiO_2-Si multilayer structures', Appl. Phys. Lett., 1986, **49** (1), pp. 13–15
4. Russell, P. St.J.,: 'Photonic Crystal Fibers', Science, 2003, **299** (5605), pp. 358–362
5. Owen, J. F., Barber, P. W., Messinger, B. J., Chang, R. K.: 'Determination of optical-fiber diameter from resonances in the elastic scattering spectrum', Opt. Lett., 1981, **6** (6), pp. 272–274
6. Ashkin, A., Dziedzic, J. M., Stolen, R. H.: 'Outer diameter measurement of low birefringence optical fibers by a new resonant backscatter technique', Appl. Optics, 1981, **20** (13), pp. 2299–2303
7. Bukshtab, M. A., Mulvad, H. C. H., Slavik, R., Poletti, F., Richardson, D. J.: 'On the Possibility of Structural Characterisation of Hollow Core Fibres using Whispering Gallery Modes Excited by Laser and Broadband Light', CLEO-E Conf., Munich, Germany, June 2019, CE-5-4
8. Frosz, M. H., Pennetta, R., Enders, M. T., Ahmed, G., Russell, P. St.J.: 'Non-invasive Real-time Characterization of Hollow-core Photonic Crystal Fibres Using Whispering Gallery Mode Spectroscopy', CLEO-E Conf., Munich, Germany, June 2019, CJ-3-6
9. Knight, J. C., Cheung, G., Jacques, F., Birks, T. A.: 'Phase-matched excitation of whispering-gallery-mode resonances by a fiber taper', Opt. Lett., 1997, **22** (15), pp. 1129–11131
10. Yariv, A.: 'Universal relations for coupling of optical power between microresonators and dielectric waveguides', Electron. Lett., 2000, **36** (4), pp. 321–322
11. Poletti, F.: 'Nested antiresonant nodeless hollow core fiber', Opt. Express, 2014, **22** (20), pp. 23807–23828
12. Bukshtab, M.: 'Photometry, Radiometry, and Measurements of Optical Losses' (Springer-Nature, Singapore, 2019, second edition)
13. Suchkov, S. V., Sumtesky, M., Sukhorukov, A. A.: 'Reflectionless potentials for slow whispering gallery modes in surface nanoscale axial photonic fiber resonators', Opt. Lett., 2015, **40** (16), pp. 3806–3809
14. Knight, J. C., Driver, H. S. T., Hutcheon, R. J., Robertson, G. N.: 'Core-resonance capillary-fiber whispering-gallery-mode laser', Opt. Lett., 1992, **17** (18), pp. 1280–1282
15. Louyer, Y., Meschede, D., Rauschenbeutel, A.: 'Tunable whispering-gallery-mode resonators for cavity quantum electrodynamics', Phys. Rev. A, 2005, **72**, Article 031801
16. Bradley, T. D., Hayes, J. R., Chen, Y., et al.: 'Record Low-Loss 1.3dB/km Data Transmitting Antiresonant Hollow Core Fibre,' Proc. ECOC Conf., 1 (2018)
17. Belardi, W. and Knight, J. C.: 'Hollow antiresonant fibers with reduced attenuation', Opt. Lett., 2014, **39** (7), pp. 1853–1856